Mechanism of catalysis, E2 recognition, and autoinhibition for the IpaH family of bacterial E3 ubiquitin ligases

Alexander F. A. Keszei[a,b] and Frank Sicheri[a,b,c,1]

[a]Lunenfeld-Tanenbaum Research Institute, Mount Sinai Hospital, Toronto, ON, Canada M5G 1X5; [b]Department of Molecular Genetics, University of Toronto, Toronto, ON, Canada M5S 3E1; and [c]Department of Biochemistry, University of Toronto, Toronto, ON, Canada M5S 1A8

Edited by Brenda A. Schulman, St. Jude Children's Research Hospital, Memphis, TN, and approved December 19, 2016 (received for review July 14, 2016)

IpaH enzymes are secreted bacterial effectors that function within host cells as E3 ubiquitin (Ub) ligases. Catalytic activity is imparted by a conserved novel E3 ligase (NEL) domain that is unique to Gram-negative pathogens and whose activity is repressed by a flanking substrate-binding leucine-rich repeat (LRR) domain when substrate is absent. How the NEL domain catalyzes the conjugation of Ub onto substrates, recognizes host E2s, and maintains its autoinhibited state remain poorly understood. Here we used mutagenesis and enzyme kinetic analyses to address these gaps in knowledge. Mutagenesis of conserved residues on two remote surfaces of the NEL domain identified functional clusters proximal to and distal to the active site cysteine. By analyzing the kinetics of Ub charging and discharging, we identified proximal active site residues that function as either the catalytic acid or catalytic base for aminolysis. Further analysis revealed that distal site residues mediate the direct binding of E2. In studying the full-length protein, we also have uncovered that IpaH family autoinhibition is achieved by a short-circuiting mechanism wherein the LRR domain selectively blocks productive aminolysis, but not the nonproductive discharge of Ub from the E3 to solvent. This mode of autoinhibition, which is not shared by the HECT domain ligase Smurf2, leads to the unanticipated depletion of E2∼Ub and thus a concomitant dominant-negative effect on other E3s in vitro, raising the possibility that short circuiting also may serve to restrict the function of host E3s in cells.

IpaH family | bacterial E3 ubiquitin ligase | ubiquitin | host-pathogen

Posttranslational modification by the covalent attachment of the small protein ubiquitin (Ub) onto lysine side chains of target proteins is an essential eukaryotic modification that imparts a wide range of consequences to the substrate, from targeting to the proteasome for degradation to the assembly of signaling complexes (1, 2). Ubiquitination begins with an E1 enzyme, which activates Ub through the consumption of ATP to form a thioester E1∼Ub adduct on its catalytic cysteine. The E1∼Ub conjugate then transthiolates Ub to the active-site cysteine of an E2 enzyme to form an E2∼Ub adduct. Finally, the charged E2∼Ub then collaborates with a diverse group of E3 ligases to catalyze the stable attachment of Ub to the ε-amino group of side-chain lysine residues or, in some cases, the N-terminal amino group of protein substrates via an aminolysis reaction.

E3 ligases can be divided into two groups based on whether or not they use a catalytic cysteine to form an E3∼Ub intermediate. The HECT (homologous to E6AP C-terminus), RBR (RING-in-between-RING), and IpaH (invasion-plasmid antigen H) families of structurally distinct E3 ligases use a catalytic cysteine residue to accept activated Ub in the form of an E3∼Ub thioester adduct. The E3 itself then catalyzes the aminolysis reaction to form an isopeptide bond between Ub and the acceptor lysine substrate. In contrast, the RING (really interesting new gene)-related E3s lack a catalytic cysteine and instead stimulate the ability of the E2 itself to catalyze aminolysis between the E2-conjugated Ub and the acceptor lysine substrate through an allosteric mechanism (3). Thus, the process of ubiquitination can be visualized as a series of activation and transthiolation reactions that terminate with a common catalytic aminolysis step.

Because Ub has seven lysine residues (and a free amino terminus), iterative action of the Ub cascade can form poly-Ub chains of various linkage topologies and lengths (1, 2), resulting in a diverse repertoire of biological outcomes. Recent structures of various enzymatic intermediates of the Ub cascade for E1, E2, RING, HECT, and RBR proteins provide a strong groundwork for understanding how these classes of eukaryotic enzymes function normally and how they are dysregulated during disease (4–7).

Ub and Ub-like modifications are heavily involved in proper immune function and regulation (8, 9). Therefore, preventing or diverting Ub signaling is a common strategy used by invasive pathogens to facilitate infection (10). Toward this end, pathogenic Gram-negative bacteria use specialized secretion systems to deliver effector proteins into the host cell as a means of manipulating Ub signaling in diverse ways. For example, the protein kinase OspG binds to and is activated by E2∼Ub conjugates, thereby competing for the availability of charged E2 (11, 12); the deamidase OspI modifies UBC13, hindering its ability to function as an E2 for the immune-related E3 ligase TRAF6 (13); the methyltransferase NleE modifies zinc-coordinating cysteine residues on TAB2 and TAB3, preventing its ability to bind K63-linked Ub chains and promote NF-κB signaling (14); and the E3 ligases SopA, a structural mimic of HECT-class E3 ligases (15), and AvrPtoB, a structural mimic of RING-class E3 ligases (16), both subvert the Ub proteasome pathway to target host proteins for destruction. Along these lines, the IpaH family is a group of conserved effector proteins found in numerous Gram-negative pathogens that subvert the host Ub pathway through their ability to function as an E3 ligase (17). Identification of in vivo targets for several *Shigella* IpaH members have revealed a recurring theme of suppression of the host

Significance

Gram-negative pathogens use a specialized secretion system to inject effector proteins into host cells to facilitate infection. Members of the IpaH family are a conserved group of effector proteins that function in the host cell as novel E3 ubiquitin ligases. How these ligases carry out their enzymatic function and how they autoregulate remain unclear. Using targeted mutagenesis, we uncover the specific function of IpaH conserved residues in E3 Ub ligase activity, either directly in the catalytic mechanism or in the recruitment of the upstream E2 enzyme. Comparison of autoinhibitory properties between IpaH members and the HECT-class E3 ligase Smurf2 reveals that IpaH enzymes short circuit the levels of charged E2 in vitro, which has the potential to subvert host ubiquitination during pathogenesis.

Author contributions: A.F.A.K. and F.S. designed research; A.F.A.K. performed research; A.F.A.K. and F.S. analyzed data; and A.F.A.K. and F.S. wrote the paper.

The authors declare no conflict of interest.

This article is a PNAS Direct Submission.

[1]To whom correspondence should be addressed. Email: sicheri@lunenfeld.ca.

This article contains supporting information online at www.pnas.org/lookup/suppl/doi:10.1073/pnas.1611595114/-/DCSupplemental.

inflammasome and innate immune responses (18) through, for example, ubiquitination of GLMN by IpaH7.8 (19) or of NEMO by IpaH9.8 (20).

IpaH enzymes catalyze aminolysis via a novel E3 ligase (NEL) domain (17, 21–23), which, despite the lack of any structural similarity to the HECT and RBR classes of E3 ligases, proceeds through an analogous IpaH~Ub thioester intermediate to generate Ub chains (17). IpaH members have a conserved two-domain architecture consisting of (*i*) a C-terminal NEL domain, which fully recapitulates E3 ligase activity in its isolated form, and (*ii*) an N-terminal leucine-rich repeat (LRR) domain, which serves the dual function of binding specific substrates for ubiquitination and autoinhibiting the constitutive activity of the NEL domain in the absence of a bound substrate (23, 24). Structures of isolated IpaH1.4 NEL domain (22), full-length autoinhibited IpaH members IpaH3 (21) and SspH2 (23), and substrate-bound complexes of SspH1-PKN1 (25) and SlrP-Trx (26) have provided an initial understanding of substrate recognition and the mechanism underlying IpaH activation. However, many functional questions remain, particularly for how IpaH E3 ligases recognize host E2 enzymes, how they catalyze aminolysis, and how precisely autoinhibition of NEL domain activity is achieved. Laying the groundwork for future structural and functional studies, here we report the mechanism of IpaH autoinhibition and provide a systematic interrogation of conserved regions within the NEL domain, elucidating the function of specific residues underlying catalysis and E2 recognition.

Results

Surface Conservation Identifies Two Functionally Relevant Interfaces. To identify functionally relevant residues involved in NEL domain E3 ligase activity, we mapped conservation onto the surface of the representative *Shigella* IpaH1.4 NEL domain structure (22) (Fig. 1*A*), substituting the better functionally characterized IpaH9.8 (20) residue numbering scheme (Fig. S1; 99% identity to the IpaH1.4 NEL domain). This exercise highlighted two clusters of surface conservation, one surrounding the active site cysteine (C337), and another distal to the active site (Fig. 1*A*). Conserved residues in the vicinity of the catalytic cysteine included R292, E338, D339, R340, R387, D397, and E400. The most highly conserved of these (D339 and D397) were previously validated as essential for IpaH function (21, 22), but their specific functions and those of surrounding residues in catalysis have not been addressed. Conserved residues at the distal region included Y487 and R508, neither of which has been functionally probed by mutagenesis.

To ascertain the functional importance of conserved residues at both spatially distinct regions, we generated point mutations within the IpaH9.8 NEL domain and quantitatively tested each point mutant for its effect on in vitro polyubiquitination activity using fluorescein-labeled Ub (Fig. 1*B*). Mutations of D339 and D397 caused a dramatic loss of activity, as expected. Surprisingly, however, mutations at surrounding conserved positions, including R292, E338, R340, R387, and E400, showed no striking effect on ubiquitination activity (Fig. 1*B*; active site cluster). We reasoned that D339 and D397 play direct roles in catalyzing aminolysis, given their proximity to the catalytic cysteine. Mutations at positions on the distal site cluster also showed defects in poly-Ub formation, with the Y487K mutation having a more pronounced effect relative to the R508D mutation (Fig. 1*B*; distal cluster). Based on the large separation in space between the distal and catalytic clusters (~30 Å), we hypothesized that the distal cluster residues play an indirect role in aminolysis, possibly by composing the E2 binding site.

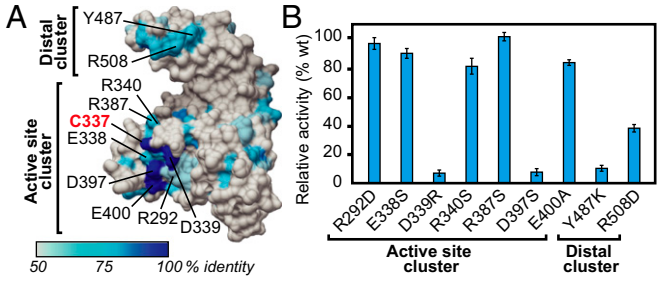

Fig. 1. Mutational analysis of conserved residues on the IpaH9.8 NEL domain. (*A*) Surface representation of the IpaH1.4 NEL domain (PDB ID code 3CKD) (22), numbered using the IpaH9.8 sequence, color-coded by conservation according to the key. Residues mutated in this study are indicated in black with the catalytic cysteine indicated in red. Conserved interfaces are grouped into active site and distal site clusters. (*B*) Catalytic E3 Ub ligase activity of IpaH9.8 NEL domain mutants relative to the WT enzyme in vitro ($n = 3$).

D339 Functions as a Catalytic Acid and D397 Functions as a Catalytic Base in IpaH9.8 Aminolysis. In general (and as best worked out for E2 enzymes), aminolysis between Ub charged onto an E2 or E3 enzyme and a lysine acceptor involves general acid-base catalysis (27–31). Within the active site, a catalytic base acts to deprotonate the incoming substrate lysine to promote its nucleophilic potential. Then, during the nucleophilic attack on the Ub~enzyme thioester bond, a catalytic acid acts to stabilize the developing negative charge of the tetrahedral transition-state intermediate (Fig. S2). The participation of specific residues in either function can be discerned by assaying the effect of mutation on the penultimate steps of Ub thioester charging and discharging of the E2/E3 enzyme and on Ub–acceptor bond formation. For example, mutation of the catalytic base can allow apparently normal E3~Ub charging and discharging, but with a failure to form Ub chains owing to a lack of nucleophilic activation of the substrate lysine (27–30). In this context, an outwardly normal Ub discharge reaction in the absence of a deprotonated lysine acceptor can be achieved via nucleophilic attack by solvent molecules, yielding nonproductive hydrolysis. Importantly, the resultant defect in aminolysis can be partially rescued by the nonspecific deprotonation of an attacking lysine side chain through an increase in the solution pH (30). In contrast, mutation of the catalytic acid produces an exaggeratedly more stable E3~Ub/E2~Ub intermediate owing to impaired discharge function resulting from insufficient stabilization of the tetrahedral intermediate formed by an attacking nucleophile (27–29). This defect is apparent in the presence of an efficiently deprotonated lysine (in the case of substrate attack) or water (in the case of nonproductive hydrolysis).

To discern the specific function of conserved active site residues in IpaH9.8 E3 ligase activity, we developed NEL domain Ub charging and discharging assays. To this end, we premixed E1 and E2 with ATP and Ub to enable steady-state formation of covalently charged E1~Ub and E2~Ub intermediates (Fig. 2*A*, *Top*, lane 1). We then assessed IpaH charging by adding wild-type (WT) IpaH9.8 NEL domain to the prepared mixture and visualizing the appearance of new molecular weight species corresponding to the NEL~Ub intermediate and poly-Ub products over time (Fig. 2*A*, *Top*, lanes 2–4). Ubiquitinated products were distinguished from thioester intermediates by running equal reaction volumes in the presence and absence of reducing agent, which selectively breaks down thioester but not isopeptide bonds, thereby allowing identification of the NEL~Ub intermediate (Fig. 2*A*, *Top*). Coinciding with the appearance of the NEL~Ub intermediate, we observed a concomitant loss of E2~Ub species, indicating that transthiolation from E2 to E3 occurs more rapidly than Ub transthiolation from E1 to E2 under our reaction conditions (indicating that E1 is limiting). Furthermore, the NEL~Ub intermediate did not accumulate beyond the first time point (1 min), indicating that the NEL~Ub intermediate rapidly achieved steady state.

Discharge analysis was then initiated by spiking EDTA into the reaction mix to inhibit E1 function, thereby preventing further activation of free Ub. The addition of EDTA led to loss of the NEL~Ub intermediate within the first time point tested (2 min), indicating that the NEL~Ub conjugate is rapidly discharged/consumed when using a WT IpaH NEL domain (Fig. 2*A*, *Top*, lanes 5–7). In contrast to the WT enzyme, the IpaH active site mutant

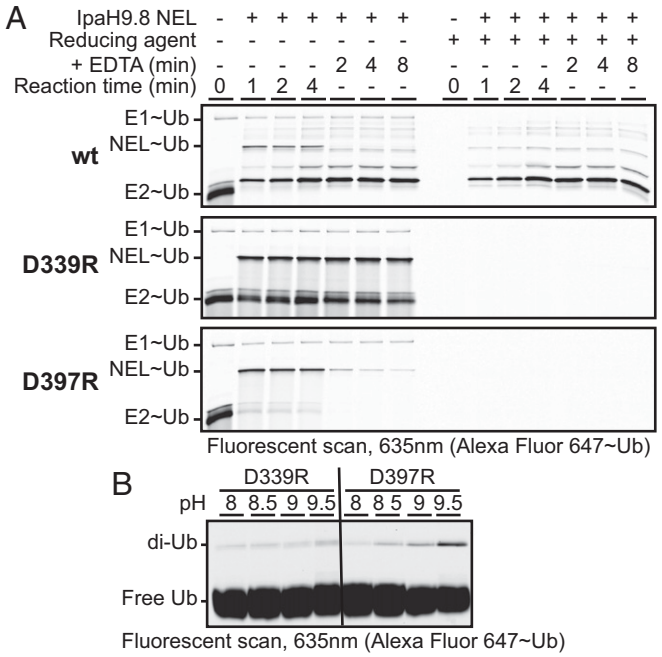

Fig. 2. Functional analysis of active site mutants. (*A*) Kinetics of Ub charging and discharging for the indicated WT (wt) and mutant IpaH9.8 NEL domains. (*B*) Effect of pH on the residual catalytic activity of indicated IpaH9.8 NEL domain mutants in vitro.

D339R (Fig. 2*A*, *Middle*) showed rapid and efficient NEL~Ub charging, but was severely compromised for discharge function. This correlated with stabilization of the E2~Ub conjugate at all time points, possibly owing to saturation of the NEL domain in its Ub-charged state, which would prevent further transthiolation from E2~Ub. In contast, the active site mutant D397R behaved more like the WT protein (Fig. 2*A*, *Bottom*), displaying outwardly normal charging and discharging activities despite a lack of aminolysis activity.

Taken together, these mutational results support a model in which D397 functions as a catalytic base and D339 functions as a catalytic acid. To further validate these inferences, we measured the effect of pH on the residual activity of D339 and D397 mutants. Consistent with only D397 functioning as a catalytic base, the D397R mutant, but not the D339R mutant, showed a partial rescue of aminolysis with an increase in solution pH (Fig. 2*B*).

Distal Residues Mediate E2 Binding. The clustering of functionally important conserved residues at a position distal from the active site strongly suggested an indirect contribution toward catalytic chemistry, such as by mediating interaction with the E2 enzyme or positioning of substrate. To elucidate the specific function of distal site residues, we tested both Y487K and R508D mutants in our NEL~Ub charging and discharging assay. In contrast to the behavior of WT enzyme (Fig. 3*A*, *Top*), both Y487K and R508D mutants (Fig. 3*A*, *Middle* and *Bottom*) yielded little to no detectable NEL~Ub species, which was further correlated by the findings of no appreciable change in E2~Ub levels. These results are reminiscent of the behavior of HECT domain mutants defective for E2 binding, which exhibit a loss of E2-E3 transthiolation and thus stabilization of the E2~Ub conjugate in charging assays (32).

To directly test whether binding of the IpaH9.8 NEL domain with its cognate E2, UBCH5B, was hindered by either Y487K or R508D mutations, we tested both WT and NEL mutants for interaction with fluorescent-labeled UBCH5B by microscale thermophoresis (MST) (Fig. 3*B*). The WT NEL domain produced significant thermophoretic shifts, yielding an estimated dissociation constant (K_d) of 185 μM (Fig. 3*B*, blue curve). This is comparable to previous reports measuring the binding of free NEL domain to the E2 enzyme by fluorescent polarization (22). Directly supporting a functional role for the conserved distal site in E2 binding, the R508D mutant displayed a ≥4-fold reduction in affinity for E2 (Fig. 3*B*, orange curve; K_d ≥670 μM), whereas the Y487K mutant showed even greater loss of affinity (Fig. 3*B*, gray curve; K_d not determined). Importantly, the relative severity of the R508D and Y487K mutants in E2 binding correlated well with their respective loss of ubiquitination activity (Fig. 1*B*, distal cluster). We conclude that the conserved distal site on the NEL domain is an E2-binding surface.

The Mechanism of Action of IpaH9.8 Is Generalizable to Other IpaH Family Members. The IpaH family member SspH1 from *Salmonella* shares only ~40% identity of its NEL domain with that of IpaH members from *Shigella*. To determine whether our insight into the catalytic mechanism of IpaH9.8 extends to SspH1 as well, we generated and characterized the corresponding mutations in full-length SspH1 (Fig. S3). Assessment of poly-Ub chain formation revealed that four residues in SspH1 (D494, D552, Y642, and R663, corresponding to residues D339, D397, Y487, and R508 in IpaH9.8) and two conserved residues in the vicinity of the catalytic cysteine (E493 and R495) are critical for function (Fig. S3*B*). To assess how these residues contribute to catalytic function, we tested all six SspH1 mutants for NEL~Ub charging and discharging kinetics. The mutants D494R, D552R, Y642K, and R663D in SspH1 demonstrated charging and discharging defects comparable to those of the corresponding mutants D339R, D397R, Y487K, and R508D, respectively, in IpaH9.8 (Fig. S3*C*, panels 2–5). The E493S and R495S mutants (Fig. S3*C*, panels 6 and 7) behaved similarly to the D494R mutant in this assay, suggesting that they cooperate with D494 in the stabilization of the tetrahedral intermediate formed during nucleophilic attack. Taken together, these findings confirm that our insight into the catalytic mechanism of IpaH9.8 extends to SspH1 and likely, more generally, to all IpaH family members as well.

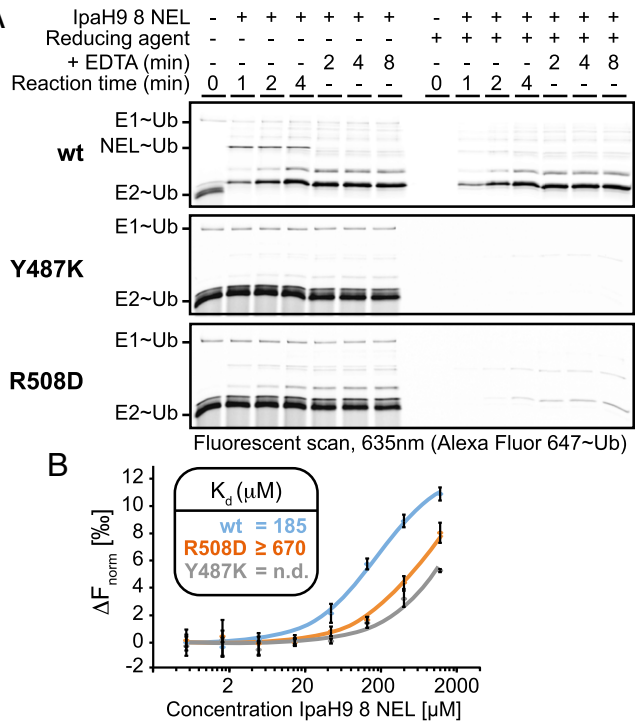

Fig. 3. Functional analysis of distal site mutants. (*A*) Kinetics of Ub charging and discharging for the indicated WT (wt) and mutant IpaH9.8 NEL domains. (*B*) Binding analysis of UBCH5 to the indicated WT or mutant IpaH9.8 NEL domains using MST. (*Inset*) Calculated K_d values (n = 3).

BIOCHEMISTRY

Autoregulation Short Circuits the NEL~Ub Charged Intermediate. Intramolecular interactions between the substrate-binding LRR domain and catalytic NEL domain restrict unbridled IpaH Ub ligase activity (23, 24). Engagement of substrate by the LRR domain relieves autoinhibition by competitively displacing interactions between the LRR and NEL domains (25). Comparing the structures of autoinhibited and isolated NEL domains suggests that autoinhibition is achieved by limiting accessibility of the catalytic cysteine, thereby preventing charging to form the NEL~Ub intermediate (21–24). Direct biochemical evidence supporting this model is lacking, however.

To shed light on the mechanism of autoinhibition, we purified full-length IpaH9.8 and tested Ub charging and discharging kinetics. Consistent with expectations, when full-length IpaH9.8 (IpaH9.8^{FL}) was added to a mixture of precharged E1~Ub and E2~Ub, no charged IpaH9.8^{FL}~Ub intermediate was detected (Fig. 4*A*, *Top*). Unexpectedly, however, the addition of IpaH9.8^{FL} to the reaction mix coincided with a wholesale loss of the E2~Ub intermediate (Fig. 4*A*, *Top*), raising the possibility that transthiolation of Ub from E2 to E3 was in fact occurring.

We reasoned that the absence of a detectable IpaH9.8^{FL}~Ub intermediate might be due to a rapid, nonproductive discharge of Ub to solvent. To explore this possibility, we tested the effect of the discharge-deficient mutant D339R in the context of the full-length enzyme. In this experiment, the D339R mutant caused the same instability of the E2~Ub intermediate, but now with detectable formation of the elusive IpaH9.8^{FL}~Ub intermediate (Fig. 4*A*, *Bottom*). Surprisingly, the D339R IpaH9.8^{FL}~Ub intermediate was more unstable than the D339R IpaH9.8^{NEL}~Ub intermediate (Fig. 2*A*, *Middle*), suggesting that autoinhibitory interactions involving the LRR domain may potentiate the nonproductive discharge of Ub.

To first confirm that the WT full-length IpaH enzyme forms an E3~Ub thioester intermediate followed by rapid hydrolysis, we used experimental conditions reoptimized to favor detection of the WT E3~Ub thioester intermediate, i.e., higher (E2) and lower temperatures (Fig. 4*B*; quantification in Fig. S4*A*). Under these conditions, we observed rapid formation and depletion of the IpaH9.8^{FL}~Ub intermediate (Fig. 4*B*, *Top*) and rapid formation but slow depletion of the IpaH9.8 ^{NEL}~Ub intermediate (Fig. 4*B*, *Bottom*). These results establish that full-length IpaH9.8 is fully competent for charging, but that the thioester-linked Ub intermediate is rapidly discharged by a short-circuiting mechanism involving nonproductive hydrolysis. Similar analyses demonstrated that the short-circuiting mechanism applies to SspH1 as well (Fig. S4 *B* and *C*).

In the foregoing experiments, the full-length enzyme consistently displayed a faster rate of thioester discharge compared with the isolated NEL domain (Fig. 4*B*; quantification in Fig. S4*A*). This difference in E3~Ub stability was recapitulated when we used a catalytic Cys-to-Ser mutational strategy to enhance detection of the E3~Ub intermediate (Fig. S4*D*). We reasoned that the apparent increase in Ub thioester discharge of full-length enzyme can be explained by the fact that the autoinhibitory state promotes E3~Ub hydrolysis. To explore this possibility, we compared the rate of hydrolysis in the presence and absence of substrate, because substrate will competitively displace autoinhibitory interactions and thus mimic the status of an isolated NEL domain with a low hydrolysis rate. To avoid the complicating effect of substrate addition on the stimulation of aminolysis, we introduced the catalytic base mutation (D552S or R) into the full-length and isolated NEL domains of SspH1 to disable aminolysis activity while leaving the hydrolysis reaction intact (Fig. S3*C*, panel 3). As expected, full-length SspH1^{D552S} demonstrated a much more rapid rate of hydrolysis than the isolated NEL^{D552R} domain (Fig. 4*C*, *Top* vs. *Bottom*). On the addition of substrate (PKN1 HR1b subdomain), no significant change in the rate of hydrolysis was observed for the full-length enzyme (Fig. 4*C*, *Middle*), indicating that autoinhibition does not promote hydrolysis per se, but rather a high rate of hydrolysis is a constitutive feature of both the active and autoinhibited states of the full-length IpaH enzyme. We conclude that

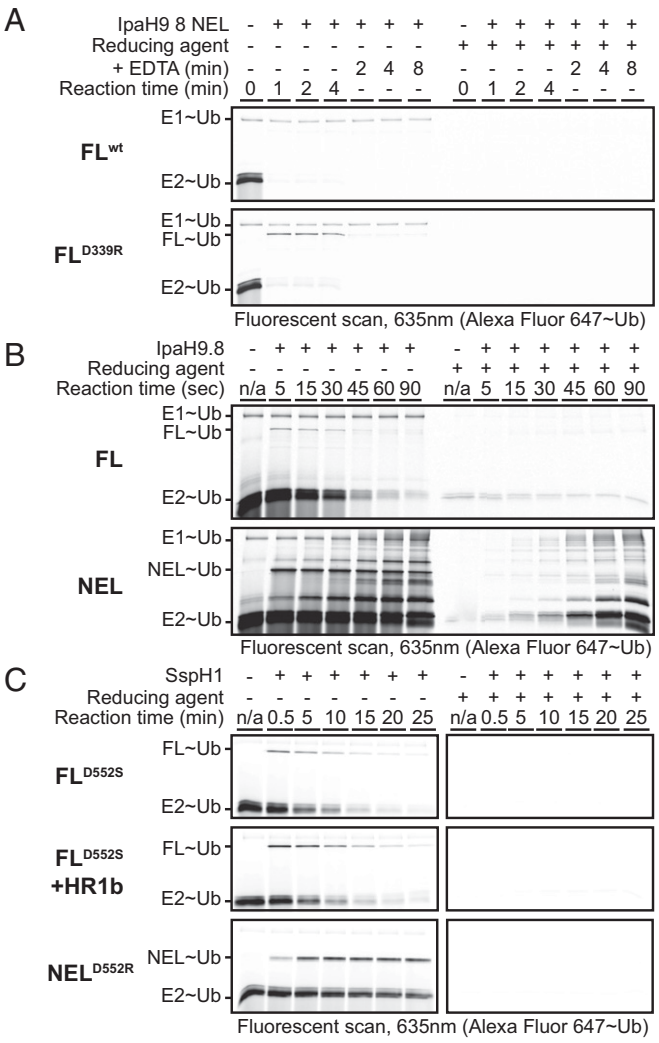

Fig. 4. IpaH autoinhibition involves a short-circuit mechanism. (*A*) Kinetics of Ub charging and discharging for WT (wt) or discharge mutant (D339R) full-length (FL) autoinhibited IpaH9.8. (*B*) Kinetics of Ub charging and discharging for WT FL and isolated NEL domain of IpaH9.8. (*C*) Kinetics of Ub charging and discharging for catalytic base (D552) mutants of FL and isolated NEL domain of SspH1 in the presence or absence of the substrate, PKN1 fragment HR1b (HR1b).

autoinhibition is achieved by the selective blockade of aminolysis activity in a manner that leaves Ub charging function and the discharge function by nonproductive hydrolysis unperturbed. Furthermore, we attribute the apparent difference in hydrolysis rates of the IpaH full-length and isolated NEL domain proteins to an intrinsic difference in the overall catalytic efficiency of the two enzyme constructs. Providing a possible explanation for the selective blocking of aminolysis over Ub charging and nonproductive hydrolysis functions, inspection of autoinhibited IpaH structures identified the loop region harboring the catalytic base as the primary point of contact for the LRR domain (Fig. S5). Thus, selective perturbation of the catalytic base would allow for an off-state that blocks aminolysis while leaving the hydrolysis function intact.

Comparison of IpaH Autoregulation with the Eukaryotic HECT Class E3 Ligase Smurf2. Smurf2 is a HECT class E3 ligase that shares several characteristics with the IpaH family: (*i*) both form Ub charged intermediates via a catalytic cysteine (1, 17), and (*ii*) both demonstrate autoinhibition by the intermolecular association of flanking regulatory domains (23, 24, 33, 34). To examine how

autoregulation differs between these two classes of E3 ligases, we characterized the kinetic properties of autoinhibited full-length Smurf2 and its constitutively active isolated HECT domain. Using a similar Ub charging and discharging assay as that used for IpaH enzymes in this study, we found that full-length Smurf2 had no significant effect on E1~Ub or E2~Ub levels and showed no evidence of charging to form a Smurf2~Ub intermediate (Fig. 5*A*, *Top*). As expected, the isolated HECT domain showed evidence of charging, but without apparent perturbation of the steady-state levels of E2~Ub (Fig. 5*A*, *Bottom*). The latter observation suggests that unlike what was observed for IpaH proteins, one or more aspects of Smurf2 HECT domain function were rate-limiting (e.g., transthiolation from the E2, catalysis of aminolysis, or Ub hydrolysis from the E3). These results indicate that the short-circuit mechanism of autoinhibition used by IpaH9.8 and SspH1 is not used by the HECT ligase Smurf2.

The observation that IpaH9.8, but not Smurf2, can efficiently deplete steady-state levels of E2~Ub conjugates in our in vitro ubiquitination reactions suggested that autoinhibited IpaH9.8 might be able to exert a dominant-negative effect on Smurf2 function if the two enzymes were mixed in reactions lacking IpaH substrate. To explore this possibility, we mixed increasing amounts of full-length autoinhibited IpaH9.8 with a fixed level (2 μM) of isolated Smurf2 HECT domain. On its own, the Smurf2 HECT domain displayed robust ubiquitination activity (Fig. 5*B*, lanes 1–3); however, as the level of autoinhibited IpaH9.8 was increased, a potent concomitant loss of Ub chain formation by the Smurf2 HECT domain was observed (Fig. 5*B*, lanes 7–9). This dominant-negative effect was also observed when using SspH1 (Fig. S6*A*) and is consistent with an autoinhibitory mechanism for IpaH enzymes involving a continuous discharge of Ub from the E3 after transthiolation from E2.

The observation that IpaH members potently deplete UBCH5~Ub pools in vitro raised the possibility that autoinhibited IpaH enzymes might suppress host ubiquitination through depletion of UBCH5~Ub pools in cells. To test this possibility, we assessed the levels of UBCH5 and UBCH5~Ub in whole-cell lysates from HEK-293 cells transfected with plasmid alone or with plasmid expressing WT or a catalytically dead mutant of SspH1 (C492A). No discernable effect on the total level of Ub-charged UBCH5 was observed across all treatment groups (Fig. S6*B*), indicating that short circuiting does not influence the global level of UBCH5~Ub in cells.

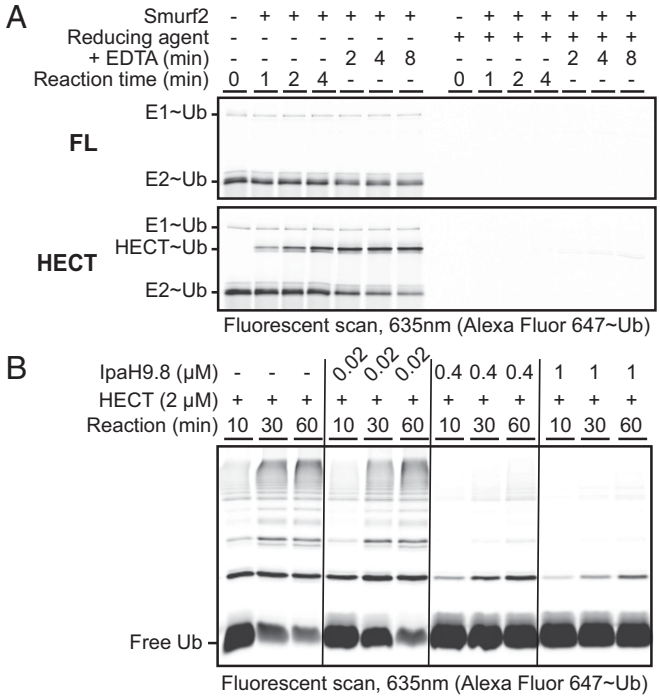

Fig. 5. The short-circuit mechanism of autoinhibition used by IpaH9.8 is not used by Smurf2 and produces a dominant-negative effect on other E3s. (*A*) Kinetics of Ub charging and discharging for full-length Smurf2 (FL) or its isolated HECT domain. (*B*) Dominant-negative effect of autoinhibited IpaH9.8 on the Ub ligase activity of constitutively active Smurf2 HECT domain in vitro.

Discussion

A worldwide increase in microbial drug resistance, coupled with stagnant growth in the discovery of new antibiotics, underscores the need for novel therapeutic approaches to directly target pathogenesis (35–37). The IpaH family, with its high conservation across numerous pathogenic Gram-negative bacteria, is an attractive candidate for the development of mechanism-based inhibitors with possibly broad applicability (18). Here we used mutational analysis of residues conserved through evolution to examine the mechanisms underlying catalysis and autoregulation for IpaH family members from *Shigella* and *Salmonella*. The insights gained may help inform future therapeutic strategies to fight bacterial infections. In addition, our study has uncovered an unanticipated mechanism by which IpaH enzymes may modulate the host Ub machinery beyond their ability to target host proteins for ubiquitination, namely by depleting the pool of charged E2s.

Eukaryotic E2 and E3 ligases share many similarities in catalyzing aminolysis despite their significant differences in structure. By analyzing the effect of mutations within the vicinity of the active site cysteine on catalysis, Ub charging, and Ub discharging kinetics, specific residues for E2 enzymes (acting in conjunction with RING E3 ligases) have been assigned functional roles as either catalytic bases or catalytic acids in aminolysis (27, 28). Although the catalytic mechanisms of the RBR (30, 38, 39) and HECT (29, 40) classes of E3 ligases are less well understood, the mutagenic results accumulated to date are consistent with specific side chains functioning analogously. Our mutational, biochemical, and enzymologic analyses of conserved residues in the IpaH family NEL domain are suggestive of a similar approach to aminolysis despite overt differences in catalytic domain structure and flanking domain architecture. Atomic structures of catalytic intermediates, such as the NEL~Ub conjugate, will be highly instructive for explaining how exactly the residues characterized in this study support enzyme function. Our work also has revealed that the full-length enzyme has greater hydrolytic activity than the isolated NEL domain, suggesting that the LRR domain or the LRR-NEL interdomain linker may contribute in some way to NEL domain catalytic function, possibly by providing supporting contacts to the conjugated donor Ub or by affecting NEL domain stability and dynamics. Additional structures of full-length catalytic intermediates may explain the basis for this effect.

A previous study probing the binding interaction between the E2~Ub intermediate and IpaH NEL domain identified an extended contact surface on the E2~Ub conjugate spanning both the E2 and the covalently attached Ub (41). This contact surface differed considerably from the contact surface on the E2~Ub conjugate used for engaging HECT domains (32). Our study has identified likely residues on the reciprocal contact surface of the NEL domain for E2~Ub interaction that combines the catalytic cysteine and a remote conserved surface located 24–28 Å away. Elucidation of the atomic structure of an E2-NEL domain complex will provide valuable information on how these two reciprocal interaction surfaces come together to support the transthiolation reaction.

E3 ligases are regulated through diverse mechanisms; for example, the multi-subunit Cullin RING E3 ligases are regulated by posttranslational modification with NEDD8 (42), the HECT-class E3 ligase Smurf2 is regulated by intramolecular interactions between the HECT domain and its flanking N-terminal C2 domain (33), and the RBR-class E3 ligase HHARI is regulated by intramolecular interactions between the RBR module and its flanking C-terminal Ariadne domain (43). Not surprisingly, the IpaH family of E3 ligases, many of which are also regulated, have a completely

different mechanism of autoregulation. Our work reveals that autoinhibited IpaH enzymes are not static entities completely deficient in all catalytic functions, but instead represent an active "short-circuited" state whereby Ub is efficiently transferred from E2 to the NEL domain and rapidly discharged nonproductively to solvent. This mode of autoinhibition may reflect a bacterial adaptation to achieve the dual goal of suppressing unwanted formation of poly-Ub chains in the absence of substrate while also depleting the local pool of charged E2s to subvert the cellular function of other E3 enzymes. Although we found that the IpaH family member SspH1 did not short circuit the global cellular pool of charged UBCH5 in cells, we cannot rule out the possibility that short-circuiting occurs more locally in the cell, for example, in the immediate vicinity of the bacterial vacuole (44) or in smaller subcellular compartments to which specific IpaH enzymes localize, such as at the apical plasma membrane in the case of SspH2 (23) and within the nucleus in the case of IpaH9.8 (45) or SspH1 (46). Further work is needed to prove that this described function of IpaH enzymes in vitro is exploited for virulence in vivo.

Materials and Methods

Detailed information is provided in *SI Materials and Methods*. Recombinant proteins were expressed from *Escherichia coli* and purified as described previously (25, 47, 48). Fluorescent labeling of indicated proteins was adapted from a previous report (47). Ubiquitination reactions were performed largely as described previously (25), with proteins visualized by fluorescence using a Typhoon FLA 9500 imager (GE Healthcare). Ub charging and discharging assays were performed similarly to the ubiquitination assays, but at 4 °C or 16 °C. Analysis of E2 charging in cells was adapted from previous work (25) by treating HEK-293 lysate with 1.35 M β-mercaptoethanol or not, as indicated, and running samples on BIS-Tris SDS/PAGE gels under neutral pH. MST-binding assays were carried out using fluorescent-labeled UBCH5B mixed with indicated amounts of IpaH9.8 NEL domain, with measurements made with a Monolith NT.Automated device (NanoTemper Technologies).

ACKNOWLEDGMENTS. This work was supported by Canadian Institutes of Health Research Grants FDN-143277 and MOP-57795 (to F.S.) and by Natural Sciences and Engineering Research Council Postgraduate Scholarship PGSD3-426371-2012 (to A.F.A.K.).

1. Komander D, Rape M (2012) The ubiquitin code. *Annu Rev Biochem* 81(1):203–229.
2. Yau R, Rape M (2016) The increasing complexity of the ubiquitin code. *Nat Cell Biol* 18(6):579–586.
3. Pruneda JN, et al. (2012) Structure of an E3:E2~Ub complex reveals an allosteric mechanism shared among RING/U-box ligases. *Mol Cell* 47(6):933–942.
4. Streich FC, Jr, Lima CD (2014) Structural and functional insights to ubiquitin-like protein conjugation. *Annu Rev Biophys* 43:357–379.
5. Berndsen CE, Wolberger C (2014) New insights into ubiquitin E3 ligase mechanism. *Nat Struct Mol Biol* 21(4):301–307.
6. Popovic D, Vucic D, Dikic I (2014) Ubiquitination in disease pathogenesis and treatment. *Nat Med* 20(11):1242–1253.
7. Buetow L, et al. (2015) Activation of a primed RING E3-E2-ubiquitin complex by noncovalent ubiquitin. *Mol Cell* 58(2):297–310.
8. Park Y, Jin H-S, Aki D, Lee J, Liu Y-C (2014) The ubiquitin system in immune regulation. *Adv Immunol* 124:17–66.
9. Fritah S, et al. (2014) Sumoylation controls host anti-bacterial response to the gut invasive pathogen *Shigella flexneri*. *EMBO Rep* 15(9):965–972.
10. Tanner K, Brzovic P, Rohde JR (2015) The bacterial pathogen-ubiquitin interface: Lessons learned from *Shigella*. *Cell Microbiol* 17(1):35–44.
11. Grishin AM, et al. (2014) Structural basis for the inhibition of host protein ubiquitination by *Shigella* effector kinase OspG. *Structure* 22(6):878–888.
12. Pruneda JN, et al. (2014) E2~Ub conjugates regulate the kinase activity of *Shigella* effector OspG during pathogenesis. *EMBO J* 33(5):437–449.
13. Sanada T, et al. (2012) The *Shigella flexneri* effector OspI deamidates UBC13 to dampen the inflammatory response. *Nature* 483(7391):623–626.
14. Zhang L, et al. (2011) Cysteine methylation disrupts ubiquitin-chain sensing in NF-κB activation. *Nature* 481(7380):204–208.
15. Diao J, Zhang Y, Huibregtse JM, Zhou D, Chen J (2008) Crystal structure of SopA, a *Salmonella* effector protein mimicking a eukaryotic ubiquitin ligase. *Nat Struct Mol Biol* 15(1):65–70.
16. Janjusevic R, Abramovitch RB, Martin GB, Stebbins CE (2006) A bacterial inhibitor of host programmed cell death defenses is an E3 ubiquitin ligase. *Science* 311(5758):222–226.
17. Rohde JR, Breitkreutz A, Chenal A, Sansonetti PJ, Parsot C (2007) Type III secretion effectors of the IpaH family are E3 ubiquitin ligases. *Cell Host Microbe* 1(1):77–83.
18. Ashida H, Sasakawa C (2016) *Shigella* IpaH family effectors as a versatile model for studying pathogenic bacteria. *Front Cell Infect Microbiol* 5:100.
19. Suzuki S, et al. (2014) *Shigella* IpaH7.8 E3 ubiquitin ligase targets glomulin and activates inflammasomes to demolish macrophages. *Proc Natl Acad Sci USA* 111(40):E4254–E4263.
20. Ashida H, et al. (2010) A bacterial E3 ubiquitin ligase IpaH9.8 targets NEMO/IKKgamma to dampen the host NF-kappaB-mediated inflammatory response. *Nat Cell Biol* 12(1):66–73, 1–9.
21. Zhu Y, et al. (2008) Structure of a *Shigella* effector reveals a new class of ubiquitin ligases. *Nat Struct Mol Biol* 15(12):1302–1308.
22. Singer AU, et al. (2008) Structure of the *Shigella* T3SS effector IpaH defines a new class of E3 ubiquitin ligases. *Nat Struct Mol Biol* 15(12):1293–1301.
23. Quezada CM, Hicks SW, Galán JE, Stebbins CE (2009) A family of *Salmonella* virulence factors functions as a distinct class of autoregulated E3 ubiquitin ligases. *Proc Natl Acad Sci USA* 106(12):4864–4869.
24. Chou Y-C, Keszei AFA, Rohde JR, Tyers M, Sicheri F (2012) Conserved structural mechanisms for autoinhibition in IpaH ubiquitin ligases. *J Biol Chem* 287(1):268–275.
25. Keszei AFA, et al. (2014) Structure of an SspH1-PKN1 complex reveals the basis for host substrate recognition and mechanism of activation for a bacterial E3 ubiquitin ligase. *Mol Cell Biol* 34(3):362–373.
26. Zouhir S, et al. (2014) The structure of the Slrp-Trx1 complex sheds light on the autoinhibition mechanism of the type III secretion system effectors of the NEL family. *Biochem J* 464(1):135–144.
27. Plechanovová A, Jaffray EG, Tatham MH, Naismith JH, Hay RT (2012) Structure of a RING E3 ligase and ubiquitin-loaded E2 primed for catalysis. *Nature* 489(7414):115–120.
28. Dou H, Buetow L, Sibbet GJ, Cameron K, Huang DT (2012) BIRC7-E2 ubiquitin conjugate structure reveals the mechanism of ubiquitin transfer by a RING dimer. *Nat Struct Mol Biol* 19(9):876–883.
29. Kamadurai HB, et al. (2013) Mechanism of ubiquitin ligation and lysine prioritization by a HECT E3. *eLife* 2:e00828.
30. Stieglitz B, et al. (2013) Structural basis for ligase-specific conjugation of linear ubiquitin chains by HOIP. *Nature* 503(7476):422–426.
31. Dou H, Buetow L, Sibbet GJ, Cameron K, Huang DT (2013) Essentiality of a non-RING element in priming donor ubiquitin for catalysis by a monomeric E3. *Nat Struct Mol Biol* 20(8):982–986.
32. Kamadurai HB, et al. (2009) Insights into ubiquitin transfer cascades from a structure of a UbcH5B approximately ubiquitin-HECT^{NEDD4L} complex. *Mol Cell* 36(6):1095–1102.
33. Wiesner S, et al. (2007) Autoinhibition of the HECT-type ubiquitin ligase Smurf2 through its C2 domain. *Cell* 130(4):651–662.
34. Mari S, et al. (2014) Structural and functional framework for the autoinhibition of Nedd4-family ubiquitin ligases. *Structure* 22(11):1639–1649.
35. World Health Organization (2014) *Antimicrobial Resistance: Global Report on Surveillance* (World Health Organization, Geveva, Switzerland).
36. Bassetti M, Merelli M, Temperoni C, Astilean A (2013) New antibiotics for bad bugs: Where are we? *Ann Clin Microbiol Antimicrob* 12:22.
37. Allen RC, Popat R, Diggle SP, Brown SP (2014) Targeting virulence: Can we make evolution-proof drugs? *Nat Rev Microbiol* 12(4):300–308.
38. Dove KK, Stieglitz B, Duncan ED, Rittinger K, Klevit RE (2016) Molecular insights into RBR E3 ligase ubiquitin transfer mechanisms. *EMBO Rep* 17(8):1221–1235.
39. Lechtenberg BC, et al. (2016) Structure of a HOIP/E2~ubiquitin complex reveals RBR E3 ligase mechanism and regulation. *Nature* 529(7587):546–550.
40. Maspero E, et al. (2013) Structure of a ubiquitin-loaded HECT ligase reveals the molecular basis for catalytic priming. *Nat Struct Mol Biol* 20(6):696–701.
41. Levin I, et al. (2010) Identification of an unconventional E3 binding surface on the UbcH5~Ub conjugate recognized by a pathogenic bacterial E3 ligase. *Proc Natl Acad Sci USA* 107(7):2848–2853.
42. Read MA, et al. (2000) Nedd8 modification of cul-1 activates SCF(beta(TrCP))-dependent ubiquitination of IkappaBalpha. *Mol Cell Biol* 20(7):2326–2333.
43. Duda DM, et al. (2013) Structure of HHARI, a RING-IBR-RING ubiquitin ligase: autoinhibition of an Ariadne-family E3 and insights into ligation mechanism. *Structure* 21(6):1030–1041.
44. Huang J, Brumell JH (2014) Bacteria-autophagy interplay: A battle for survival. *Nat Rev Microbiol* 12(2):101–114.
45. Toyotome T, et al. (2001) *Shigella* protein IpaH$_{(9.8)}$ is secreted from bacteria within mammalian cells and transported to the nucleus. *J Biol Chem* 276(34):32071–32079.
46. Haraga A, Miller SI (2003) A *Salmonella enterica* serovar typhimurium translocated leucine-rich repeat effector protein inhibits NF-κ B-dependent gene expression. *Infect Immun* 71(7):4052–4058.
47. Huang H, et al. (2014) E2 enzyme inhibition by stabilization of a low-affinity interface with ubiquitin. *Nat Chem Biol* 10(2):156–163.
48. Ogunjimi AA, et al. (2005) Regulation of Smurf2 ubiquitin ligase activity by anchoring the E2 to the HECT domain. *Mol Cell* 19(3):297–308.
49. Bond CS, Schüttelkopf AW (2009) ALINE: A WYSIWYG protein-sequence alignment editor for publication-quality alignments. *Acta Crystallogr D Biol Crystallogr* 65(Pt 5):510–512.
50. Sievers F, et al. (2011) Fast, scalable generation of high-quality protein multiple sequence alignments using Clustal Omega. *Mol Syst Biol* 7:539.
51. Pettersen EF, et al. (2004) UCSF Chimera: A visualization system for exploratory research and analysis. *J Comput Chem* 25(13):1605–1612.